Quaternary Science Reviews 45 (2012) 18–30

Contents lists available at SciVerse ScienceDirect

Quaternary Science Reviews

journal homepage: www.elsevier.com/locate/quascirev

Glacial outburst floods and loess sedimentation documented during Oxygen Isotope Stage 4 on the Columbia Plateau, Washington State

Eric V. McDonald [a,1], Mark R. Sweeney [b,*], Alan J. Busacca [c,2]

[a] Desert Research Institute, Division of Earth and Ecosystem Sciences, 2215 Raggio Parkway, Reno, NV 89512-1095, USA
[b] University of South Dakota, Earth Sciences, 414 E. Clark Street, Vermillion, SD 57069, USA
[c] Vinitas Consultants LLC, P.O. Box 822, White Salmon, WA 98672, USA

ARTICLE INFO

Article history:
Received 14 July 2011
Received in revised form
7 March 2012
Accepted 9 March 2012
Available online 30 May 2012

Keywords:
Loess
Channeled Scabland
Cordilleran ice sheet
Late Pleistocene
Pacific Northwest

ABSTRACT

Stratigraphy and age control of late Pleistocene loess, associated glacial outburst flood deposits and flood-cut unconformities in the Channeled Scabland, Washington State, United States, indicate a significant Cordilleran ice sheet advance during marine Oxygen Isotope Stage 4. Glacial outburst flood deposits from stage 2 (classic Bretz flood deposits, ca 21 to 13 ka) and related features in the Channeled Scabland overlie a widespread layer of loess that contains buried soils and the Mount St. Helens set C tephra (ca 46 ka). This loess in turn overlies deposits of the penultimate episode of giant outburst floods and an unconformity cut by those floods. Regional trends in the thickness, texture, and overall composition of the older loess are strikingly similar to those from the youngest loess, known to be derived from stage 2 flood deposits. We conclude that the older loess also is derived from fine-grained flood deposits. Luminescence ages, tephrochronology, and soil development rates indicate that the bulk of deposition of the older loess occurred during stage 3, following glacial outburst flooding marked by a regional flood-cut unconformity. The apparent cyclical pattern of cold-climate buried soils, flood deposits, and thick loess accumulations demonstrate that sediment supply renewed by flood episodes is a major control on accumulation of loess on glacial timescales.

1. Introduction

Loess deposits in the Channeled Scabland and Palouse in Washington State (Fig. 1) provide a proxy record of advances of the Cordilleran ice sheet and related glacial outburst floods that have inundated the Channeled Scabland in multiple episodes for the last 2 Ma (Patton and Baker, 1978; Waitt, 1985; McDonald and Busacca, 1988; Bjornstad et al., 2001; Pluhar et al., 2006; Baker, 2009). The most recent episode of Channeled Scabland flooding occurred during the latest Pleistocene (marine Oxygen Isotope Stage 2; hereafter stage 2) and has been well-documented, especially the connections between the advance of the Cordilleran ice sheet, formation of glacial Lake Missoula, and the timing of Channeled Scabland floods (also commonly called the Missoula Floods or the Bretz Floods) that occurred between ca 21 to 13 ka (Bretz, 1969; Waitt and Thorson, 1983; Waitt, 1985; Atwater, 1986; Benito and O'Connor, 2003; Clague et al., 2003; Lopes and Mix, 2009; Hanson et al., 2012). A regional stratigraphic framework for late Pleistocene loess composed of loess layers, correlative buried soils, glacial flood stratigraphy, and tephrochronology suggests a possible stratigraphic connection between the two most recent loess layers and the two most recent episodes of Channeled Scabland flooding (Fig. 2; McDonald and Busacca, 1992; Busacca and McDonald, 1994). The youngest of these loess layers (informally named L1) regionally overlies both deposits and flood-cut unconformities related to the well-documented late Wisconsin episode of outburst floods from glacial Lake Missoula. The older, underlying loess layer (informally named L2) also overlies deposits and flood-cut unconformities that have been interpreted to be related to the penultimate episode of Channeled Scabland floods. Subsequent luminescence dating of the loess indicates that deposition of the L2 loess layer likely began in the later part of stage 4 (Berger and Busacca, 1995; Richardson et al., 1997) which occurred between about 74 and 58 ka (Martinson et al., 1987; Mix, 1992).

Existing geochronology and stratigraphy of the loess (Fig. 2) suggest that the penultimate episode of Channeled Scabland flooding is related to glacial outburst floods generated from stage 4 (early Wisconsin) glacial advances of the Cordilleran ice sheet;

---

* Corresponding author. Tel.: +1 605 677 6142; fax: +1 605 677 6121.
E-mail addresses: Eric.McDonald@dri.edu (E.V. McDonald), Mark.Sweeney@usd.edu (M.R. Sweeney), alan@vinitas.net (A.J. Busacca).
[1] Tel.: +1 775 673 7302.
[2] Tel.: +1 509 592 0756.

0277-3791/$ – see front matter © 2012 Elsevier Ltd. All rights reserved.
doi:10.1016/j.quascirev.2012.03.016

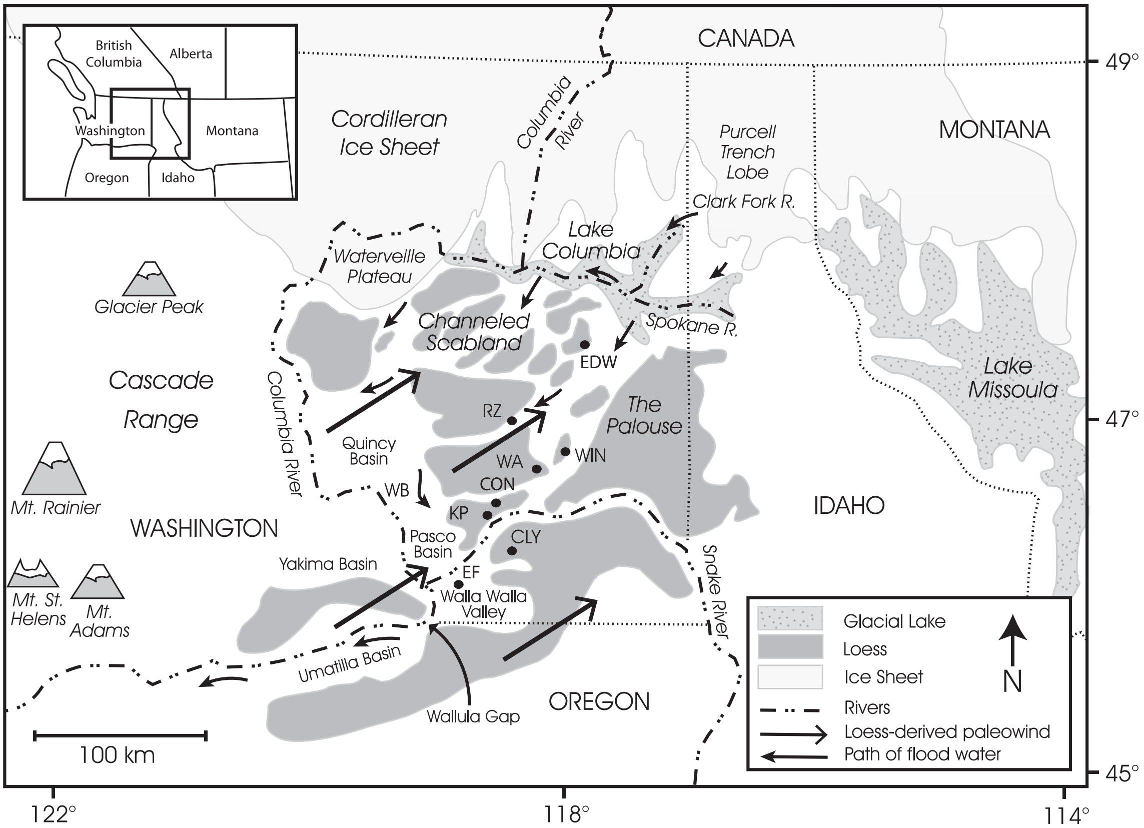

Fig. 1. Location map of the Pacific Northwest showing the glacial Lake Missoula-Channeled Scabland system, the Cordilleran ice sheet at its late Wisconsin maximum, loess deposits, prevailing winds, and generalized flood flow directions. Abbreviations for sites referenced in text and figures: CLY-1/2 (CLY), Con-1 & 2 (CON), EDW-1 (EDW), KP-1 (KP), RZ-1 (RZ) WA-5 & 9 (WA), WIN-1 (WIN), and White Bluffs (WB).

however, several important questions remain. First, flood deposits within the Channeled Scabland and glacial Lake Missoula system that can be directly attributed to stage 4 glaciation have not been positively identified or dated. Second, although pre-Frasier glacial deposits in British Columbia have been correlated with stage 4 Cordilleran ice (Fulton and Smith, 1978; Clague, 1989), the southern extent of this ice sheet, especially in relation to glacial lobes capable of creating a glacial Lake Missoula, remains unknown due to erosion and modification of sediments during subsequent glaciations and flood events (Booth et al., 2004). Third, other major sources of glacial outburst flood water in southern British Columbia and northern Washington may have contributed to the penultimate episode of Channeled Scabland flooding and loess generation, rather than entirely from a stage 4 glacial Lake Missoula (Shaw et al., 1999; Lesemann and Brennand, 2009). Fourth, although current geochronology of the loess in the Channeled Scabland indicates deposition began during stage 4, a regional synthesis of loess stratigraphy, geochronology, paleowind dynamics, and sources of loess and its chronologic relation to stage 4 glacial floods has yet to be demonstrated.

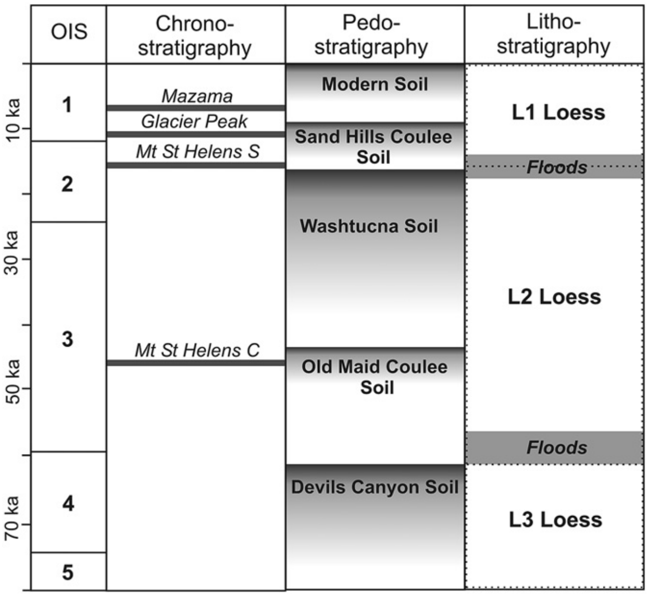

Fig. 2. Summary of regional stratigraphy including chronostratigraphic markers (tephras), pedostratigraphy (buried soils), and lithostratigraphy in relation to Oxygen Isotope Stages.

In this paper, we integrate the timing and nature of loess accumulation, glacial advances, and associated glacial outburst floods to document the connection between the L2 loess layer and stage 4 outburst flooding of the Channeled Scabland. First, we outline evidence for older flooding events that likely occurred during stage 4, including descriptions of flood-cut unconformities and flood deposits in relation to loess stratigraphy. Second, we provide evidence suggesting that prevailing dust-transporting winds have remained relatively unchanged since stage 4. Third, we demonstrate how flood slackwater sediments are compositionally similar to loess. Last, we show how luminescence ages, tephrochronology, and soil development rates of the loess help pinpoint the age of penultimate glacial outburst floods, and thus the timing of the advance of the Cordilleran ice sheet during stage 4.

2. Setting

2.1. Palouse loess

Loess covers >50,000 km^2 on the Columbia Plateau in southeastern Washington, western Idaho, and northeastern Oregon (Fig. 1). The loess is variable in thickness and mantles the Miocene-age Columbia River Basalt Group, Tertiary-age sedimentary deposits including the Ringold Formation, and Pleistocene glacial outburst flood sediments. The loess sequence is up to 75 m thick and has normal-reverse-normal polarity signatures suggesting that some of the loess is as old as 1 to 2 Ma (Busacca, 1989). Detailed luminescence dating has elucidated the timing of loess deposition in the late Pleistocene (Fig. 3; Berger and Busacca, 1995; Richardson et al., 1997, 1999).

The top of the L1 loess (ca 15 to 0 ka) is capped by the modern surface soil which is underlain by the Sand Hills Coulee Soil, a buried soil that likely formed during the latest Pleistocene to early Holocene (McDonald and Busacca, 1992; Sweeney et al., 2005). The base of the L1 contains the Mount St. Helens set S (hereafter: MSH set S) tephra at its base. The age of the MSH set S tephras are debated and include a commonly reported calibrated radiocarbon age of 15.5 ka (13,000 ^{14}C yr B.P., Mullineaux, 1986) that was recently refined to about 15.8 ka based on paleomagnetic secular variation (13,350 to 14,400 ^{14}C yr B.P., Clague et al., 2003). Luminescence ages of loess bracketing the set S support these ages (Richardson et al., 1997), as do radiocarbon ages of snails collected above the tephra in loess (Spencer and Knapp, 2010). These ages, combined with other older radiocarbon ages from numerous other deposits associated with the tephras suggest the eruptions centered around 16 ka (Clynne et al., 2008).

The L2 loess (ca ~77 to 16 ka) contains the Washtucna Soil, a well-developed buried soil, characterized by Stage III to IV carbonate morphology (Gile et al., 1966) with vertical and horizontal seams of soil carbonate in most exposures (McDonald and Busacca, 1990, 1992). Underlying the Washtucna Soil is the moderately developed Old Maid Coulee buried soil and the Mount St. Helens set C (hereafter: MSH set C) tephra. The best age estimate for the MSH set C tephra is 46.3 ± 4.8 ka (Berger and Busacca, 1995). The L2 loess overlies the next older loess unit, L3, which contains the Devils Canyon Soil at its top, a well-developed buried soil similar to the Washtucna Soil (McDonald and Busacca, 1992). The boundary between L1 and L2 loess is defined by the MSH set S tephra. In the absence of this tephra, the boundary is defined as the top of the Washtucna Soil or by the presence of glacial outburst flood sediment (McDonald and Busacca, 1992; Busacca and McDonald, 1994).

The Washtucna Soil at the top of L2 is a buried soil that formed between ca 40 and 20 ka, based on luminescence dating (Richardson et al., 1997). The carbonate morphology of this soil suggests arid to hyper-arid conditions during formation (McDonald and Busacca, 1990, 1992). The Washtucna Soil is dominated by carbonate-cemented cylindrical nodules formed by nymphs of burrowing cicadas that fed on roots of woody shrubs such as sagebrush (*Artemisia*; O'Geen and Busacca, 2001). Opal phytoliths from the Washtucna Soil record a dominance of *Artemisia* during formation of the soil (Blinnikov et al., 2002) across large areas that have supported a bunchgrass-dominant community in the Holocene, confirming that the soil formed under cold and dry conditions of the last glacial maximum (stage 2).

A similar soil structure (carbonates and cylindrical nodules) and phytolith assemblage are found within the Devils Canyon Soil at the top of L3 loess (McDonald and Busacca, 1992; Blinnikov et al., 2002). Luminescence ages on loess bracketing the Devils Canyon Soil suggest that this soil formed during the cold conditions of stage 4 (Berger and Busacca, 1995; Richardson et al., 1997).

Loess units proximal to source areas tend to fine upward and have sand-rich bases (McDonald and Busacca, 1990, 1992). The sand-rich bases often are void of soil development features, suggesting rapid accumulation. The fining-up loess units have been interpreted as related to sediment supply and availability controlled by rejuvenation of the sediment supply following a new phase of glacial outburst flooding (McDonald and Busacca, 1990; Busacca and McDonald, 1994) and also may be related to changes in wind strength.

2.2. The Channeled Scabland

Connections between the stage 2 advance of the Cordilleran ice sheet, formation of glacial Lake Missoula, and generation of floods in the Channeled Scabland have been documented extensively

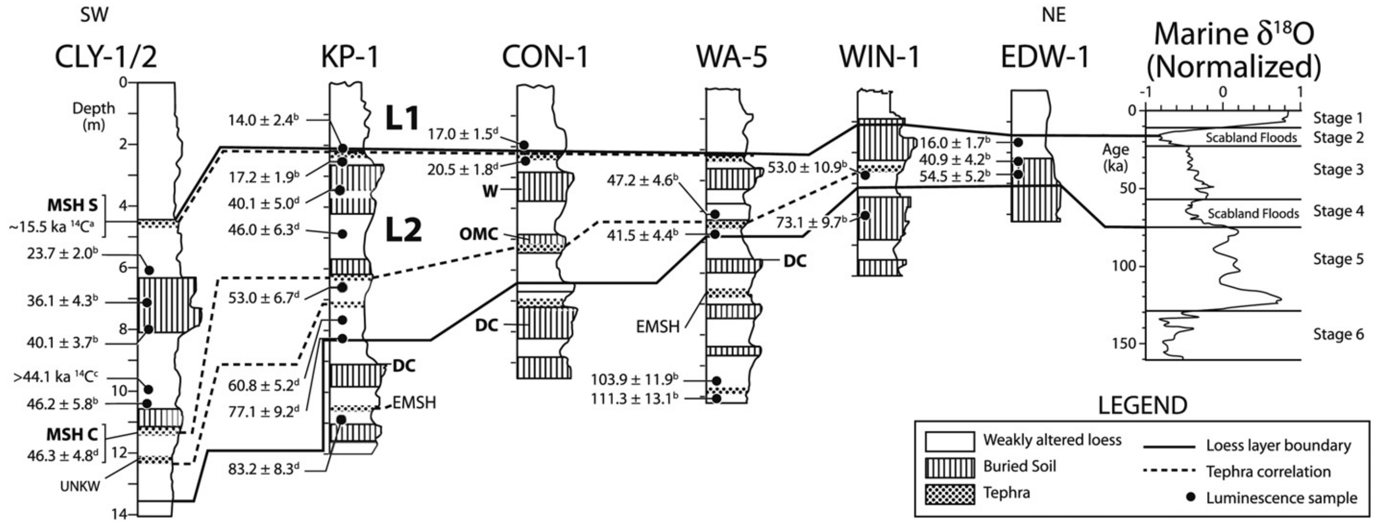

Fig. 3. Regional stratigraphic framework of late Quaternary loess (McDonald and Busacca, 1992) and correlation to normalized marine δ^{18}O curves (modified from Martinson et al., 1987). Sections are oriented proximal (CLY = upwind) to distal (EDW = downwind). Correlations are based on buried soils, tephra, and luminescence data. Superscripts following ages (in ka) aligned along left margin of stratigraphic columns indicate source: (a) calibrated ^{14}C date for MSH set S tephra; (b) thermoluminescence, Richardson et al. (1997, 1999); (c) ^{14}C date from charcoal; and (d) thermoluminescence, Berger and Busacca (1995). Abbreviations: Washtucna Soil (W), Old Maid Coulee Soil (OMC), Devils Canyon Soil (DC), Mount St. Helens C (MSH C), Mount St. Helens S (MSH S), Earlier Mount St. Helens (EMSH), and unnamed tephra (UNKW).

(Bretz, 1923, 1969; Waitt and Thorson, 1983; Baker and Bunker, 1985; Waitt, 1985; Clague et al., 2003; Baker, 2009). Glacial Lake Missoula was created when the Clark Fork River in northern Idaho was blocked by the Purcell Trench lobe of the Cordilleran ice sheet (Fig. 1). Episodic failure of this ice dam resulted in floods of different magnitude. Extensive erosion of preexisting loess along Scabland flood channels is marked by a regional unconformity that truncated and scoured soils and loess layers (sometimes mantled by flood deposits) and cut steep-sided channels through the loess (McDonald and Busacca, 1988). One of the major flood pathways was via the Cheney-Palouse Scabland tract, extending from Spokane, WA to the Pasco Basin. Many subsequent floods likely bypassed the Cheney-Palouse in favor of the lower-lying Grand Coulee once the Grand Coulee in the northwestern part of the Scabland had formed (Bretz, 1932; Patton and Baker, 1978).

Hydraulic damming of flood water at Wallula Gap, a narrow constriction along the Columbia River, generated a temporary lake that resulted in deposition of bedded, fine-grained sediment (hereafter referred to as slackwater sediments) in low-lying Pasco, Walla Walla, and Yakima basins of south-central Washington (Fig. 1). Significant gravel bars were deposited only along the main flood channels or coulees. The MSH set S tephra is commonly found in stage 2 slackwater sediments (Mullineaux et al., 1978; Waitt, 1985). Stage 2 slackwater sediment, ice-rafted debris, and other flood features can be found as high as 365 m asl, the estimated maximum height of flood waters in south-central Washington (Baker et al., 1991; O'Connor and Baker, 1992). Thin L1 loess locally mantles features created by stage 2 Scabland flooding, including erosional scarps in deep loess along flood channels, flood gravels, and flood-scoured basalt bedrock.

3. Methods

This paper integrates what is known of the regional loess stratigraphy with glacial outburst flood deposits. New soil ages, grain size data, and compositional data are presented here.

Age control was previously established using tephrochronology, luminescence, and radiocarbon. Unknown tephras in loess were geochemically fingerprinted and matched with reference tephras of known age and source (Busacca et al., 1992). Luminescence ages of loess have been published elsewhere (Berger and Busacca, 1995; Richardson et al., 1997, 1999). Ages were determined by both thermoluminescence (TL) and infrared stimulated luminescence (IRSL) methods in two different laboratories. Ages determined by the two laboratories provide somewhat different results for comparable intervals but generally are not different at 2σ. Luminescence ages are in good agreement with independent ages of tephra. An AMS-radiocarbon age on charcoal found in loess provides an internal check on luminescence ages.

In this paper, we use soil extraction methods to estimate the duration of soil formation. The amount of secondary pedogenic carbonates, an index for soil development, was determined using a Chittick device, as outlined by Machette (1985). Iron oxide accumulation within the soil, another index for soil development (McFadden and Hendricks, 1985), was determined by measuring dithionite extractable Fe-oxyhydroxides (Fe_2O_3) using atomic absorption spectrometry (Loeppert and Inskeep, 1996). Rates of accumulation of carbonate and iron oxides for buried soils within the loess were then calculated using an age of 15.5 ka for the base of the L1 loess.

Regional loess thickness data for both L1 and L2 loess (McDonald, 1987; Busacca and McDonald, 1994) were interpolated to a grid in ArcGIS 10.0 using the regularized spline method with an input of six points for each 1 km cell. The spline method fits a mathematical function to a specified number of nearest input points while passing through the sample points (Franke, 1982; Mitas and Mitasova, 1988). Thickness data was superimposed on a map showing surface geology including loess and flood deposits (Washington Division of Geology and Earth Resources, 2010).

New grain size data of loess and slackwater flood sediment was determined using a Malvern Mastersizer S, a laser diffractometer (Sperazza et al., 2004) that measures volume percent of particles from 0.05 to 850 μm. Samples were pretreated prior to analysis with sodium acetate to dissolve soil carbonates and with hydrogen peroxide to oxidize organic matter. Samples were then rinsed in deionized water, centrifuged, and decanted. Each sample was dispersed with sodium hexametaphosphate and analyzed in a deionized water suspension with no sonication. These new data were used to compare grain size properties of loess and slackwater flood sediments.

Major and trace element geochemistry of the loess and potential sources including flood slackwater, Ringold Fm. sediments, and Columbia River Basalt Group was determined by X-ray fluorescence (XRF). Bulk samples were prepared using the double-fusion method (Johnson et al., 1999). Field sampling focused on the finer-grained (<2 mm) slackwater flood and Ringold deposits that are most similar in grain size to the loess. Fifty-nine samples of L1 and L2 loess were collected from five different stratigraphic sections across the Columbia Plateau. Seven stage 2 slackwater flood samples were collected from the Pasco and Walla Walla basins for comparison. Eight Ringold Fm. samples were collected from the White Bluffs along the Columbia River. We compared our data to the Columbia River basalt data from Hooper (2000) who used a similar XRF technique.

4. Results: linking deposition of L1 and L2 loess to glacial outburst floods

4.1. Stratigraphic evidence for stages 2 and 4 glacial floods

The record of stage 2 and older floods is preserved within the loess either as flood-cut unconformities or as coarse-grained sediments (Patton and Baker, 1978; McDonald and Busacca, 1988; Bjornstad et al., 2001; Pluhar et al., 2006). Coarse-grained flood deposits can range from well-bedded gravel with foreset-beds to poorly sorted deposits of cobbles, sand, and silt.

Flood-cut unconformities preserved within the loess are primarily located in areas marginal to flood channels. Unconformities related to stage 2 flood events appear as: (1) truncation of loess and buried soils that pre-date the L1 loess, including scour features eroded into the Washtucna Soil; (2) deposition of basaltic gravel (granular size or larger) lenses within loess; and (3) deposition of ice-rafted debris (McDonald and Busacca, 1988, 1992).

Unconformities with similar features also underlie the L2 loess at several localities (Fig. 4) indicating that glacial outburst floods also generated the unconformity at the base of L2. Specific descriptions of these sites are found in McDonald and Busacca (1988, 1989), and a few of these sites are summarized below.

A road cut near Connell (CON-2; Fig. 4A) that is located within a loess island in the Washtucna Coulee contains an example of a flood-cut unconformity that is related to the penultimate episode of flooding. A prominent unconformity underlies the L2 layer that contains the Washtucna Soil and the MSH set C tephra (Line A, CON-2, Fig. 4A). The MSH set C tephra is within sediment overlying the unconformity that appears to be primarily a mixture of eolian sediment and locally reworked flood deposits indicating that deposition of the tephra occurred sometime after formation of the flood-cut unconformity. The L2 layer and Washtunca Soil are conformably overlain by L1 loess containing the MSH set S tephra. Pre-stage 4 floods are also recorded in the CON-2 exposure as

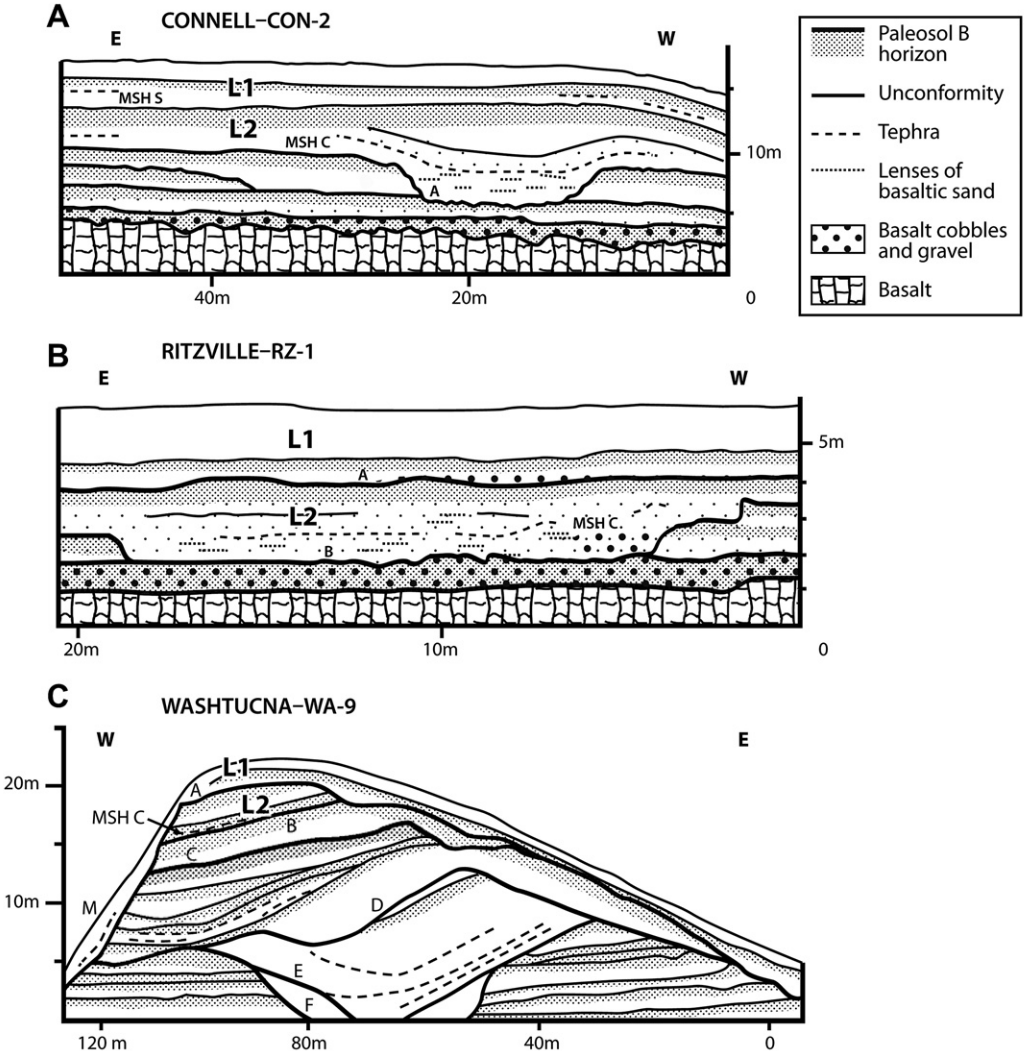

Fig. 4. Sites containing flood-cut unconformities. Letters are used to label unconformities from youngest to oldest and do not imply correlation between sites. Abbreviations: Mount St. Helens Set S tephra (MSH S), Mount St. Helens Set C tephra (MSH C), Mazama tephra (M), L1 loess (L1), and L2 loess (L2). A. Stratigraphy of Connel (CON-1) exposure lacks a stage 2 unconformity, but an unconformity roughly correlative to stage 4 (A) is overlain by MSH C. B. Stratigraphy of Ritzville (RZ-1) exposure reveals both stage 2 (A) and stage 4 (B) unconformities. C. Stratigraphy of Washtucna (WA-9) exposure reveals a long history of eolian deposition and erosion, including flood-cut unconformities at stage 2 (A) and stage 4 (B).

erosion and truncation of the underlying basalt that is overlain by flood sediment containing reworked basalt cobbles and gravel in a silt matrix. Unconformities are mantled by basalt cobbles.

A road cut near Ritzville (RZ-1, Fig. 4B) contains evidence for both stage 2 and stage 4 floods. The Washtucna Soil at the top of the L2 loess was eroded by stage 2 floods, generating an unconformity that is overlain by scattered basaltic clasts and sands (line A, Fig. 4B). This layer, in turn, is overlain by L1 loess containing MSH set S tephra. A second unconformity (line B, Fig. 4B) underlies the Washtucna and Old Maid Coulee soils. Flood-derived basalt clasts, gravel, sand, and laminated silt directly overlie the unconformity. Above these flood sediments are the L2 loess and the MSH set C tephra. The sediment containing the MSH set C may be primary flood deposits, but it is more likely that this sediment is a mixture of eolian sediment and locally reworked flood deposits. An older flood-cut surface that is mantled by cemented basalt cobbles underlies the L2 and older loess units.

The Washtucna-9 site (WA-9; Fig. 4C) is a 20-m deep road cut containing more than a dozen loess units and paleosols with multiple unconformities that truncate paleosols and loess units. The L2 loess containing the Washtucna Soil and MSH set C tephra is present above a flood-cut unconformity near the top of the road cut (line B, Fig. 4C). Stage 2 floods eroded this site producing a steep scarp along the western margin of this loess hill, truncating the Washtucna Soil and older loess. The L1 loess mantles the surface and contains the Mazama tephra (ca 7600 cal yr B.P.; Zdanowicz et al., 1999).

Upstream from Walulla Gap in Eureka Flat, several outcrops record pre-stage 2 floods (Fig. 5). At LM-1, gravel foresets are cemented at the top by calcium carbonate, capped by L1 and L2 loess. Older sedimentary outcrops on Eureka Flat contain a Mt. Rainier tephra which has an age older than the last glacial maximum (Sweeney et al., 2007). These older, tephra-bearing sediments have been truncated and are capped by flood-deposited rubble, eolian sand, and L1 loess. The flood-deposited rubble is composed of imbricated, pebble-sized nodules of carbonate-cemented loess. This rubble is correlated to the top of the Devils Canyon Soil at site PV-1, preserved below L2 loess which contains the MSH set C tephra. The rubble is interpreted as generated by stage 4 floods that overtopped the divide south of the Snake River and Palouse River confluence, sending erosive water down Eureka Flat (Fig. 5B), eroding the preexisting sediment, and

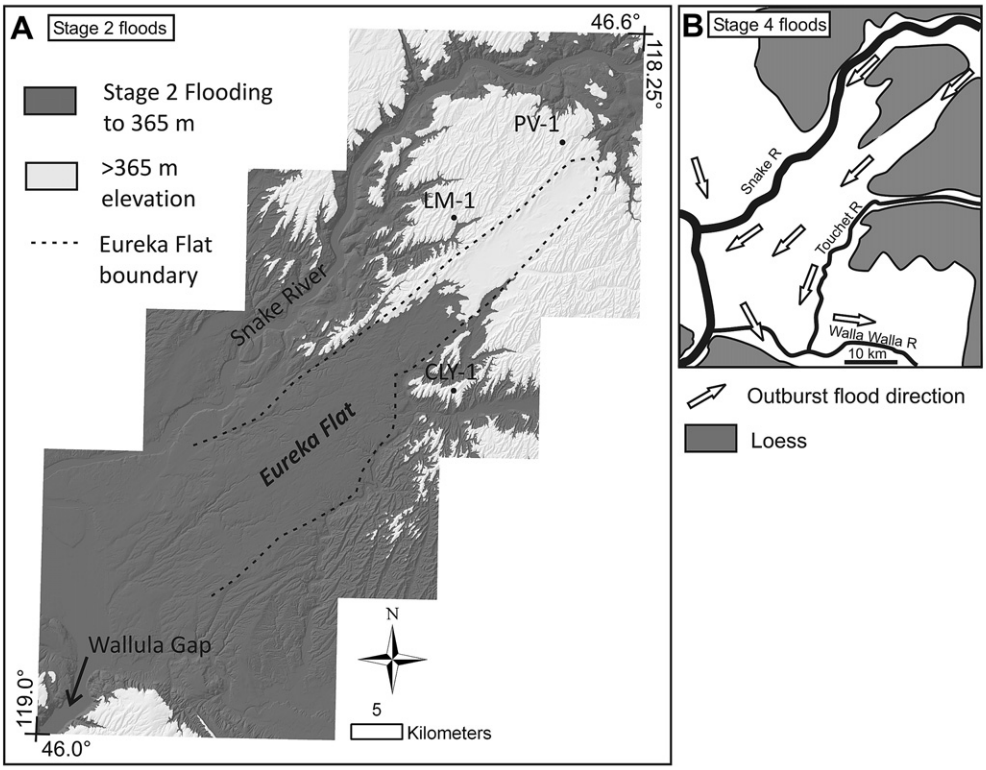

Fig. 5. Eureka Flat and localities. A. Hillshade map with dashed line depicting Eureka Flat. Dark shaded area represents maximum flood elevation of 365 m as estimated by O'Connor and Baker (1992). Area above this elevation was not inundated with flood water during stage 2 outburst floods. B. Schematic of Eureka Flat during stage 4, depicting flood waters overtopping the divide at the north end of Eureka Flat and flowing southwest to Wallula Gap. Flood-emplaced rubble from stage 4 floods is located at PV-1, and cross-bedded gravels are located at LM-1.

scouring and re-depositing carbonate-cemented soil nodules (Sweeney et al., 2007). The rubble is widespread at Eureka Flat, but only found above the maximum elevation reached by stage 2 floods, suggesting that an older episode of floods must be responsible.

Flood-cut unconformities also can be found in loess outcrops north of the Walla Walla Valley (Fig. 6). Several loess layers and buried soils that were once continuous across the landscape were eroded by Scabland floods to form rounded hills or mini loess islands. The Washtucna Soil at site EF (Fig. 6) is formed within L2 loess mantling the unconformities, which in turn is mantled by L1 loess. The location of the unconformity between the Washtucna Soil and older, truncated loess supports stage 4 flooding at this site.

4.2. Glacial-flood sediments as the source of the L1 and L2 loess

4.2.1. Regional patterns in loess layer thickness

Studies of loess in the Great Plains and Midwest regions of the U.S. have demonstrated that trends in loess thickness generally thin parallel to the prevailing paleowind directions and away from sediment sources (Frazee et al., 1970; Ruhe, 1983; Mason et al., 1994; Mason, 2001; Muhs et al., 2008). Loess accumulations tend to be thickest closest to their source area because a large proportion of the suspension load is coarse silt and very fine sand particles that only can be transported short distances (within ~10 km), while fine silt and clay particles are transported longer distances (>100 km; Pye, 1987).

Regional trends of the L1 and L2 loess thickness in the Palouse generally decrease to the northeast and downwind (discussed in more detail below) from widespread areas of flood slackwater sediment. Modeled distributions of thickest loess range from about 450 cm for the L1 to about 900 cm for the L2 marginal to Walla Walla Valley and Pasco Basin (Figs. 1 and 7). These two basins contain the most extensive deposits of fine-grained slackwater sediment because these basins were deeply flooded as a result of hydraulic damming of flood water at Wallula Gap. Regional decreases in loess layer thickness are also depicted in Fig. 3 along a series of stratigraphic exposures. The thickest loess measured is at the CLY-1/2 sites (L1: 444 cm, L2: 858 cm). Other areas that show minor local increases in loess thickness are marginal to flood deposits in the Quincy Basin and along the Cheney-Palouse Scabland tract. Regional trends displayed in Fig. 7 are generally similar to trends first documented in Busacca and McDonald (1994) using a different method of spatial analysis.

4.2.2. Paleowind evidence

Persistent south-southwesterly paleowinds are required to produce regional thinning of the L1 and L2 layers to the northwest and away from the areas of slackwater sediments. Several additional lines of evidence suggest that prevailing south-southwesterly winds have driven the eolian system of the Pacific Northwest for at least 75 kyr. General circulation models (GCMs) and regional climate models for the Pacific Northwest simulate strong southwesterly surface winds for the region since the LGM (COHMAP, 1988; Bartlein et al., 1998; Hostetler and Bartlein, 1999).

In the latest Pleistocene and Holocene, prevailing westerly to southwesterly paleowinds have been recorded by dune cross-strata and slip-face orientations across the Columbia Plateau (Lewis, 1960; Gaylord and Stetler, 1994; Gaylord et al., 2001, 2011; Sweeney et al., 2005). Eolian sand deposits from earlier in the Pleistocene have not been documented, so paleowind directions for the Pleistocene (>15 ka) must be inferred from other physical evidence, such as regional trends within the loess (see above).

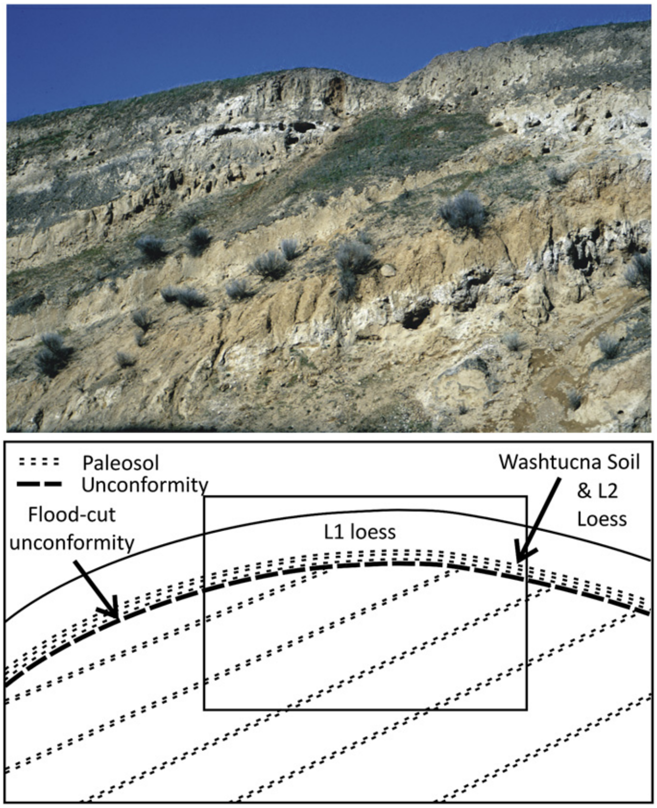

Fig. 6. Bisected hill north of Walla Walla reveals numerous loess units, each capped by a buried soil containing calcium carbonate and cicada burrow fabric similar to the Washtucna Soil. Units are truncated and capped by loess containing the Washtucna Soil that includes cicada burrow fabric and laminar carbonate, and 1.7 m of L1 loess. Elevation of locality is 405 m asl, exceeding the maximum elevation for stage 2 floods. Stratigraphic relations constrain erosion to pre-L2 loess deposition, and the scale of erosion is consistent with stage 4 flooding.

Geomorphology of the loess also provides insight into paleowind directions. Loess forms a blanket of relatively uniform thickness over preexisting topography (Pye, 1995). Some proximal loess accumulations in Europe, the Midwest U.S., and the Palouse have accumulated in linear ridges that are aligned with the prevailing wind direction (Lewis, 1960; Flemal et al., 1972; Ruhe, 1983; Leget, 1990). Formation of linear loess ridges is presumed to be caused by loess accumulating on leeward sides of topographic obstacles to the wind (Lewis, 1960; Leget, 1990), by draping of loess on preexisting linear features (Flemal et al., 1972), or by deposition and subsequent wind erosion of loess (Mason et al., 2011). Loess ridges in Washington are oriented approximately N25E to N30E, roughly parallel to the prevailing winds. The cores of the ridges reveal old loess layers and related paleosols. Initiation of linear ridge development in the Pleistocene likely began with the accumulation of loess downwind of basalt knobs (Lewis, 1960). Subsequent loess units have since blanketed the linear ridges. Considering that the linear ridges have had their present orientation throughout the entire time of their formation (likely >100 kyr), it is reasonable to assume that southwesterly winds influenced older loess accumulation as well.

Distribution of tephras within the Palouse loess provides some evidence for southwesterly to westerly winds for more than 50 kyr. Distributions of tephra record wind directions at the time of eruption, although multiple tephras produced during an eruptive phase may record seasonal shifts in wind direction (Porter, 1981). Tephra layers derived from Cascade volcanoes including Mount St. Helens sets S and C and Glacier Peak have been identified within loess and/or slackwater flood sediment at numerous locations across the Channeled Scabland and record prevailing west-southwesterly winds (Busacca et al., 1992; McDonald and Busacca, 1992).

4.2.3. *Geochemical evidence*

Early work in the Palouse recognized that the mineralogy of the loess reflected that of Cordilleran rocks north and east of the Columbia Plateau, not the Miocene Columbia River basalts that are the dominant bedrock of the region. Bryan (1927) called this the "Palouse soil problem" because the prevailing winds in the Palouse blow from the southwest and the basalt could not be the source of eolian sediment forming the "Palouse Soil" (i.e., the Palouse loess). Other potential sources located upwind of the loess that are of similar mineralogic composition include glacial outburst flood slackwater sediments and the Miocene-Pliocene Ringold Fm. The Ringold Fm. can be found exposed along the White Bluffs of the Columbia River (Fig. 1) and is interpreted to be deposited by an ancestral Columbia River (Newcomb, 1958). The Ringold Fm. lithofacies are gravel, sand, and mud-dominated, with the mud facies representing overbank and lacustrine deposits and gravels representing channel deposits (Lindsey and Gaylord, 1990).

Regional trends in the L1 and L2 loess units described above indicate that the primary source of these layers is deflation of fine-grained slackwater glacial-flood sediments; therefore, the loess should be geochemically similar to the flood sediments. No slackwater flood sediments from stage 4 have been identified in the Channeled Scabland; however, if the L1 and L2 loess units are geochemically identical, it is reasonable to conclude that the L2 loess was also derived from older slackwater sediments. McDaniel and Hipple (2010) also noted that the L1 and L2 loess are mineralogically similar except for minor differences in clay mineralogy due to weathering.

To test the hypothesis that the loess is derived from flood sediments, we compared the major and trace element composition of L1 and L2 loess samples from several sites across the Columbia Plateau to stage 2 flood slackwater sediments, Ringold Fm., and Columbia River basalt. The use of geochemical data in sedimentary provenance studies has been shown to be useful especially when comparing immobile elements (Taylor and McLennan, 1985). Provenance studies of loess and dust have utilized several key tracers including Ce, La, Nb, Rb, Sc, Th, Ti, Y, and Zr where differentiation in potential sources can be revealed on ternary diagrams or bivariate plots (Sun, 2002; Marx et al., 2005; Muhs and Benedict, 2006; Muhs et al., 2007, 2008). For example, Sc–Th–La is commonly used to differentiate upper crustal sediments and is useful in comparing loess versus basalt (Taylor and McLennan, 1985).

Ternary and bivariate plots of key major and trace elements from this study reveal that the L1 and L2 loess are compositionally similar and share the same sediment source (Fig. 8). Geochemical data clearly indicate that the Columbia River basalts are not a source of loess (Fig. 8A). By comparison, the L1 and L2 loess overlap in composition with stage 2 flood slackwater sediment and fine-grained facies of the Ringold Fm. (Fig. 8). It is not surprising that the flood and Ringold sediments are compositionally similar considering they are both derived from diverse bedrock and sediment sources within the extensive Columbia River watershed. The results suggest that both the flood and Ringold sediments could be potential sources of loess. The Ringold sediment cannot be a substantial source of loess because the Ringold Fm. is limited in extent and exposure across the Columbia Basin and in many places is capped by a resistant silicified soil (Newcomb, 1958). The combination of large geographic extent of the flood slackwater sediment and its geochemical similarity with the loess indicates that the flood sediment is the primary source for both the L1 and L2 loess.

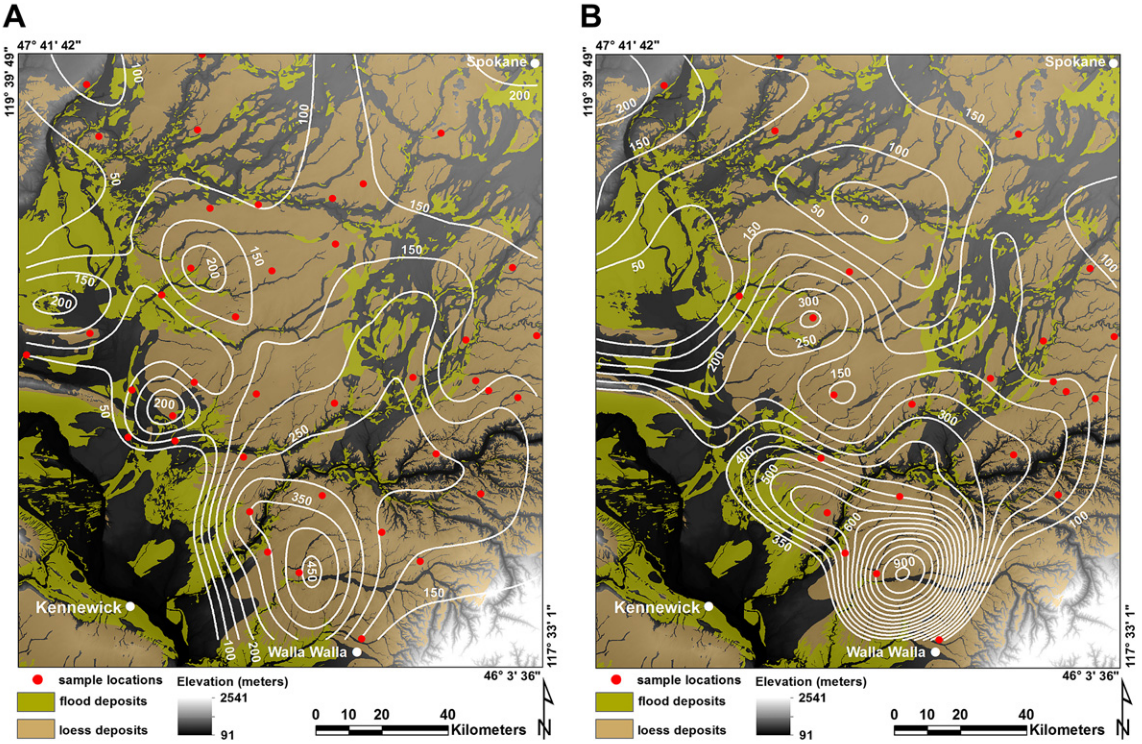

Fig. 7. Contour maps of loess thickness in cm for the L1 (A) and L2 (B) loess layers. Contour interval is 50 cm. The thickest L1 loess is immediately downwind of extensive glacial outburst flood slackwater sediments and thins northeast toward Spokane. L2 loess has a similar distribution but is much thicker.

4.2.4. Grain size evidence

Regional grain size trends in the L1 and L2 loess fine to the northeast in support of prevailing southwesterly winds. Loess across the Palouse has a silt loam texture, but proximal loess sites such as CLY-2 and KP-1 contain greater than 30% sand, whereas distal loess sites such as WIN-1 and EDW-1 contain less than 10% sand. Trends are interrupted by local sources from outburst flood coulees that result in several coarse modes of loess across the region (Busacca and McDonald, 1994). On a more local scale, fining of loess can be seen downwind of individual source areas. From a regional perspective, the main body of loess is derived from multiple flood slackwater basins (Sweeney et al., 2005), thus influencing its overall texture and thickness.

Grain size analysis of proximal L1 and L2 loess reveals striking similarity in mean size, sorting, and proportion of sand, silt, and clay to flood slackwater sediments and fine-grained facies of the Ringold Fm. (Fig. 9). Loess and flood sediment have nearly identical, overlapping grain size distributions (Fig. 9B). Short distance of transport from dust source (flood slackwater sediment) to sink (loess) can produce loess with similar textures to the source sediment because limited sorting has occurred during transport. Despite grain size similarities of loess and Ringold sediment, the Ringold is of limited extent and therefore is not likely to be a major source of the loess.

4.3. Age of the loess

Radiometric and calibrated soil ages of the L2 loess and buried soils indicate that the base of the L2 began accumulating during stage 4 and continued during stage 3 (Fig. 3). A luminescence age from the base of L2 at KP-1 indicates that loess deposition may have occurred as early as about 77 ± 9.2 ka (Berger and Busacca, 1995). Other luminescence ages for L2 loess indicate that deposition continued to about 41.5 ± 4.42 ka (WA-5, Fig. 3), followed by a decrease in accumulation rate and formation of the Old Maid Coulee Soil. A radiocarbon age of >44,030 ^{14}C yr B.P from charcoal (Beta 84504) found at the CLY-1 outcrop (Fig. 3) above the Old Maid Coulee Soil is internally consistent with bracketing luminescence ages. The presence of the MSH set C tephra (46 ka) just below or at the base of the Old Maid Coulee Soil indicates that this soil formed during stage 3. As discussed above, the MSH C tephra occurs within the base of L2 loess that accumulated just above flood-cut unconformities at WA-9, RZ-1, and CON-2. Luminescence ages on loess that stratigraphically underlie the L2 range from 83.2 ± 8.3 ka (KP-1, Fig. 3) to 73.1 ± 9.7 ka (WIN-1, Fig. 3), indicating that deposition of the L3 layer and formation of the Devils Canyon Soil occurred during in stage 5 and possibly into early stage 4.

Rates of soil development for three sites within the L2 loess support the numerical ages and a correlation to stage 4 for the base of L2 (Table 1; Fig. 3). Calcium carbonate and iron oxide accumulation in soils are both relatively well understood and used separately to determine rates of soil development, as both properties increase in soils over time (Machette, 1985; McFadden and Hendricks, 1985). We calibrated the rate of pedogenic accumulation of carbonate and dithionite extractable Fe-oxyhydroxides by scaling mass accumulation rates of these products in soils within the L1 loess. We used these rates to estimate the total time required for soil development in the L2 loess (Old Maid Coulee and Washtucna soils). Pedogenic rates based on the accumulation of soil carbonate and iron oxide indicate that the Old Maid Coulee Soil began to form about 41–69 ka, or about 28–48 ka based on extractable iron. Pedogenic-based ages for L2 loess are consistent with luminescence ages for the loess and MSH set C tephra.

5. Discussion

Regional stratigraphy and geochronology of the L2 loess indicate that the penultimate episode of glacial outburst flooding of the

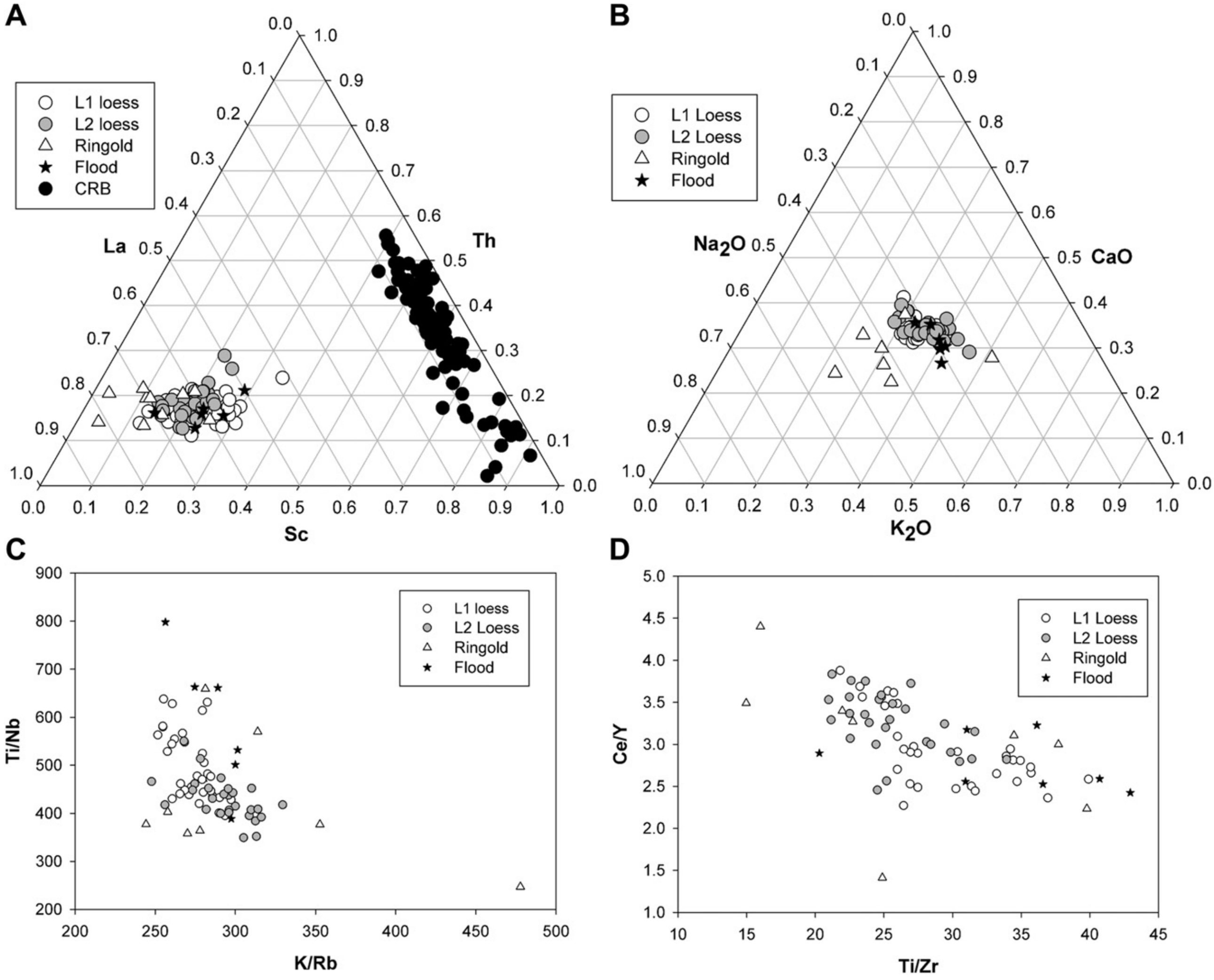

Fig. 8. Geochemistry of loess and potential sources. A. Sc–Th–La ternary plot comparing composition of Columbia River basalts to loess, flood, and Ringold sediments. Data for the Columbia River basalts is from Hooper (2000). B. Ternary plot of major oxides K_2O–CaO–Na_2O. C. Bivariate plot of K/Rb versus Ti/Nb reveals similarities between L1 & L2 loess, flood, and Ringold sediments. D. Bivariate plot of Ti/Zr versus Ce/Y comparing loess and potential sediment sources.

Channeled Scabland occurred during stage 4. First, the age of a regional flood-cut unconformity is constrained by the presence of the 46 ka MSH set C tephra that overlies this unconformity at several localities. The stratigraphic position of this unconformity generally correlates with the onset of L2 accumulation. Multiple luminescence ages from the lower sections of L2 loess range in age from about 77 to 41 ka, indicating that deposition probably coincided with stage 4 flooding and continued into stage 3. Second, luminescence ages, geochemical evidence, regional patterns in thickness of the L1 and L2 loess, and paleowind directions clearly demonstrate that deposition of both the L1 and L2 loess is connected to rejuvenation of the eolian sediment supply related to glacial outburst floods. The regional distribution pattern and stratigraphic relationships of L2 loess are noticeably similar to those of L1 (Figs. 3 and 7), indicating that L2 had a similar genesis. The L2 layer is more than 750 cm thick immediately downwind northeast of extensive slackwater sediments in basins in southern Washington and northern Oregon and thins progressively downwind to the northeast (Figs. 3 and 7). L2 has a nearly identical composition to L1 (Fig. 8) and, in locations near flood coulees, contains unconformities similar to the flood-cut unconformities found at the base of L1 (Fig. 4).

In the Palouse, major episodes of soil formation in the loess appear to have occurred primarily during full glacial conditions (Berger and Busacca, 1995; Richardson et al., 1997, 1999; McDonald and Busacca, 1998). In many other loess regions of the world, major episodes of soil formation occurred primarily during interglacials (Pye, 1995; Muhs and Bettis, 2003). This out-of-phase relationship of the timing of loess accumulation and soil formation in the Palouse compared to other areas can be explained by changes in atmospheric circulation patterns in the Pacific Northwest. During stage 2, the large North American ice sheets produced a glacial anticyclone that resulted in weakened, prevailing dust-transporting winds that decreased regional loess accumulation rates and allowed strong calcic soils to form (Sweeney et al., 2004). A return to strong onshore, westerly flow following the last glacial maximum, combined with sediment sources in basinal areas that were replenished by outburst floods, restarted the Palouse dust engine (Sweeney et al., 2004).

The current geographic distribution of loess in the Pacific Northwest can be explained by how efficiently different parts of the regional landscape were able to trap dust. Little to no L1 loess has accumulated on surfaces stripped to basalt bedrock or on top of gravel bars in the Channeled Scabland during the Holocene due to

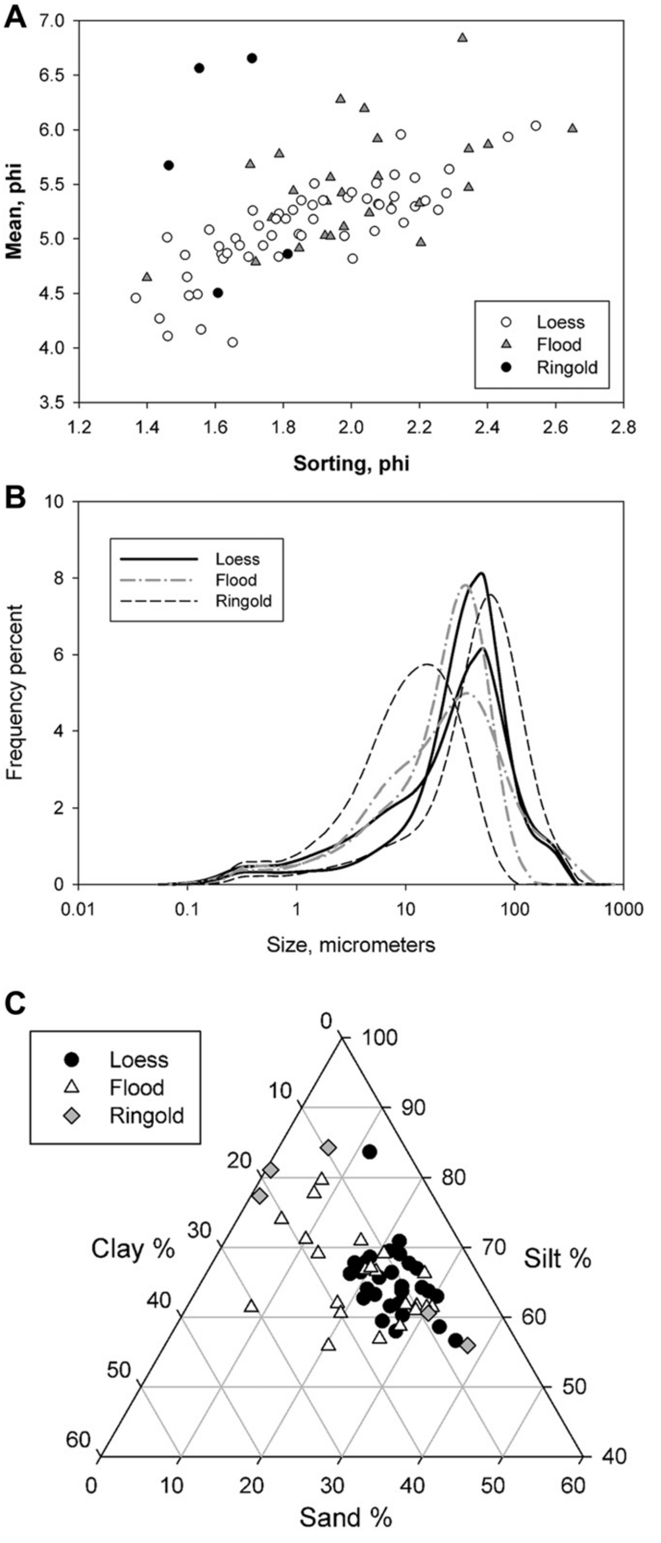

Fig. 9. Grain size data of loess and potential sources. A. Sorting versus mean shows overlap of loess and flood sediment. B. Frequency percent graphs showing the nearly identical distributions of flood and loess sediments. C. Ternary plot of percent sand, silt, and clay.

a paucity of trapping vegetation on these surfaces. Thick accumulations of loess are found on older deposits of loess where vegetation likely persisted during flood events, or in areas where vegetation could quickly colonize following outburst flooding. At the CLY-1 site, which is above the maximum elevation reached by the last flooding episode (Fig. 5), 450 cm of L1 loess accumulated (Fig. 3) (McDonald and Busacca, 1990).

Loess generation is tied directly to upwind sand dune activity (Sweeney et al., 2005, 2007). Saltating sand grains bombard the source bed, releasing dust-sized particles that are transported downwind (Bagnold, 1941; Shao et al., 1993) and deposited as loess. The upwind perimeter of the Palouse loess is surrounded by dune fields and sand sheets. For the most part, dunes and sand sheets mantle fine-grained flood sediments that are a reservoir for dust-sized particles. While clear evidence of Holocene dune activity exists that can be correlated to L1 loess formation (Gaylord and Stetler, 1994; Gaylord et al., 2001; Sweeney et al., 2005), Pleistocene-aged eolian sand deposits that would have been linked to L2 loess are difficult to find, likely because they were stripped away by catastrophic glacial outburst floods (Gaylord et al., 2003). Isolated outcrops of sand sheet deposits that pre-date stage 2 flood sediments in the southern part of the Columbia Plateau (Sweeney et al., 2007) indicate that there were eolian sands on the upwind perimeter of the L2 loess as well.

Genesis of L2 loess and flood-cut unconformities at its base requires a stage 4 advance of the Cordilleran ice sheet to trigger outburst flooding. Cosmogenic ages from glacial boulders in the Yukon Territory in northern Canada document the first stage 4 glacial advance recognized in the entire Canadian Cordillera (Ward et al., 2007). Penultimate glacial moraines in Alaska have also yielded cosmogenic ages of stage 4/early stage 3 (Briner et al., 2005). Glacial deposits that record advances of the Cordilleran ice sheet before stage 2 are rare to find east of the Cascade Range in Washington State. The bulk of evidence exists in the Puget Lowland and marine record. Glacial deposits that underlie stage 3 (about 58–25 ka; Martinson et al., 1987) interglacial sediments in western Canada usually have been assigned to the early Wisconsin (stage 4; see references in Clague, 1989; Clague et al., 1992), but these deposits could be as old as stage 6.

Amino acid and luminescence ages document pre-stage 3 glacial sediments in the Puget Lowland, some of which could represent a stage 4 advance (Blunt et al., 1987; Berger and Easterbrook, 1993; Easterbrook, 1994). Luminescence ages from the Possession Drift suggest that the Possession glacier advanced to the area of Tacoma during stage 4 (Troost et al., 2003). Weathering rinds on outwash gravels in the Puget lowland have been correlated to a stage 4 advance approximately the same size as the stage 2 Fraser glaciation (Colman and Pierce, 1992). In the eastern Cascade Range, cosmogenic dating of boulders in glacial moraines suggests that there were several Pleistocene advances of mountain glaciers, including an advance between 77 and 71 ka (Porter et al., 2005). Pollen from Carp Lake at the western margin of the Columbia Plateau suggests that conditions were colder and drier during stage 4 than present, but perhaps not as cold and dry as stage 2 (Whitlock et al., 2000). Modeling of North American ice sheet dynamics suggests that there was a spike in the Cordilleran ice sheet volume at approximately 60 ka and that the maximum ice sheet area occurred between 70 and 60 ka (Marshall et al., 2000).

Compelling evidence of stage 4 glaciation comes from the marine record. Turbidites off the west coast of Washington and Oregon have been tied directly to Pleistocene outburst flooding during stage 2 (Zuffa et al., 2000; Normark and Reid, 2003). These sediments are compositionally similar to Proterozoic rock sources that are typical of the glacial Lake Missoula area (Prytulak et al., 2006). Older turbidites have been found below stage 2 turbidites and have been estimated based on sediment accumulation rates to be as old as 55 ka (Normark and Reid, 2003) which broadly correlates to flood-cut unconformities in loess stratigraphically below the MSH Set C tephra (46 ka). In addition, new evidence from ice-

Table 1
Pedogenic rate calculations for soils in the L1 and L2 loess layers.

Site	L1					L2					Total $CaCO_3$ age (ka)[a]	Total Fe_2O_3 age (ka)[a]
	Thickness (cm)	$CaCO_3$		Fe_2O_3		Thickness (cm)	$CaCO_3$		Fe_2O_3			
		Soil (g/cm^2)	Rate: g/cm^2-kyr^{-1}	Soil (g/cm^2)	Rate: g/cm^2-kyr^{-1}		Soil (g/cm^2)	Pedogenesis length (kyr)	Soil (g/cm^2)	Pedogenesis length (kyr)		
CLY-1/2	444	28.9	1.9	3.3	0.2	858	58.3	31	5.8	28	47	43
KP-1	225	11.3	0.8	1.3	0.1	354	29.2	47	2.7	33	62	48
CON-1	218	13.7	0.9	2.0	0.1	319	33.4	36	3.0	19	52	35
WA-5	218	7.6	0.5	2.0	0.1	217	20.2	41	1.8	14	57	29
WIN-1	123	5.7	0.4	1.2	0.1	136	19.5	53	1.0	13	69	28
EDW-1	144	4.8	0.3	1.3	0.1	162	8.0	26	1.5	18	41	34

[a] Total age is pedogenesis length (kyr) of L2 summed with age of L1 (15.5 kyr).

rafted debris in marine sediments off the coast of Vancouver Island was dated at 47 ka and provides evidence for the collapse of the Cordilleran ice sheet following stage 4 (Cosma et al., 2008). Two similar, but younger, ice-rafted debris events have been correlated with the collapse of the ice sheet following the stage 2 glacial maximum (Cosma et al., 2008).

Loess stratigraphy demonstrates that initiation of L2 loess accumulation coincided with penultimate outburst floods in the Channeled Scabland indicating that an age range between about 77 and 46 ka broadly constrains the age of the penultimate advance of the Cordilleran ice sheet. This age agrees with estimates of about 74–58 ka for stage 4 glaciation from oxygen isotope records (Martinson et al., 1987) and of 75–68 ka based on SPECMAP estimates (Mix, 1992) and is also consistent with the age of the Possession Drift in the Puget Lowland (Blunt et al., 1987; Easterbrook, 1994), as well as timing for ice-rafted debris deposition (Cosma et al., 2008). Moreover, marine terrace ages suggest that sea level dropped after about 80 ka with expansion of global ice volume during stage 4 (Muhs, 1992).

The distribution, morphology, and height of flood-scoured surfaces from penultimate floods, including the regional extent of the unconformity beneath L2 loess, are similar to those from stage 2 floods indicating that the stage 2 and stage 4 glacial outburst floods were of similar magnitude. Limited field evidence suggests that stage 4 floods may have been larger than stage 2 floods along the Cheney-Palouse Scabland tract based on the stratigraphic position of flood-cut unconformities and the stage 2 Washtucna Soil. In some outcrops, the stage 4 flood-cut unconformity can be found below the Washtucna Soil, but no unconformity from stage 2 flooding exists above the soil, suggesting stage 2 floods were of lesser volume along specific pathways.

An alternative explanation involves the modification and evolution of flood pathways with each successive flood event that may have played a role in the elevation of some unconformities. The widening or deepening of flood pathways could influence the effect of successive flood events. For example, a large volume of water flowing down more constrictive flood pathways during stage 4 could have helped flood waters surpass the divide south of the Snake-Palouse River divide, allowing water to flow down Eureka Flat. Contemporaneous and later erosion of flood pathways prohibited potentially larger floods during stage 2 to take a similar path.

Despite the lack of evidence for a stage 4 glacial Lake Missoula, we hypothesize that an earlier glacial Lake Missoula was likely involved, along with other subglacial sources of water, in Scabland flooding because (1) the Cheney-Palouse Scabland tract, which is the most proximal exit path for flood waters from glacial Lake Missoula onto the Columbia Plateau, contains flood-cut unconformities from stage 4; and (2) nearly identical composition of the L1 and L2 loess suggests that the flood sediments from which these loess units were eroded were derived from similar source areas in stage 2 and stage 4. In order for a stage 4 glacial Lake Missoula to have formed, the Cordilleran ice sheet must have advanced south of the 48th parallel in order to block the drainages necessary to produce glacial Lake Missoula.

6. Conclusions

Numeric dating from the base of L2 loess in the Channeled Scabland and Palouse region of Washington constrains the age of a regional flood-cut unconformity to about 77–46 ka. The age of this unconformity is consistent with floods associated with the penultimate advance of the Cordilleran ice sheet. These ages also verify that accumulation of loess began during stage 4 and continued through stage 3 in response to increased sediment supply and availability following the penultimate episode of glacial outburst flooding. Thickness and grain size trends of L2 loess are strong evidence for prevailing southwesterly winds during the Pleistocene.

Although slackwater sediments from penultimate floods have not been identified, the striking similarity between L1 and L2 loess on the basis of distribution, thickness trends, texture, and composition indicates they had a similar genesis. The last episode of glacial outburst floods caused extensive erosion along major flood pathways and also deposited expansive sand- and silt-rich sediment in slackwater basins that has acted as a source for eolian sediments, especially loess. Penultimate floods of a similar magnitude would have left behind slackwater sediments that were deflated to produce loess but eventually eroded or buried by the next episode of flooding. The linkage between the stage 2 advance of the Cordilleran ice sheet, the generation of glacial outburst floods, and the subsequent formation of L1 loess serves as an analog to signatures of earlier ice sheet advances, floods, and loess accumulation episodes, especially during stage 4.

Acknowledgments

This work was completed with funding from the National Science Foundation (EAR 92 20012 and ATM 0214508). Preparation of this manuscript was partially funded by the Army Research Office (DAAD19-03-1-0159). Geochemical data is from the Washington State University Geoanalytical Lab. Lisa Wable and Chris Kratt assisted with drafting figures. We would like to thank John Clague, Vic Baker, and an anonymous reviewer for constructive comments on this manuscript.

References

Atwater, B.F., 1986. Pleistocene glacial-lake deposits of the Sanpoil River valley, northeastern Washington. United States Geological Survey Bulletin. 1661.

Bagnold, R.A., 1941. The Physics of Blown Sand and Desert Dunes. Chapman and Hall, London.

Baker, V.R., 2009. The channeled scabland: a retrospective. Annual Review of Earth and Planetary Science 37, 393–411.

Baker, V.R., Bunker, R.C., 1985. Cataclysmic late Pleistocene flooding from glacial Lake Missoula- a review. Quaternary Science Reviews 4, 1–41.

Baker, V.R., Bjornstad, B.N., Busacca, A.J., Fecht, K.R., Kiver, E.P., Moody, U.L., Rigby, J.G., Stradling, D.F., Tallman, A.M., 1991. Quaternary geology of the Columbia plateau. In: Morrison, R.B. (Ed.), Quaternary Nonglacial Geology: Conterminous. U. S. Geological Society of America, Boulder, pp. 215–250.

Bartlein, P.J., Anderson, K.H., Anderson, P.M., Edwards, M.E., Mock, C.J., Thompson, R.S., Webb, R.S., Webb III, T., Whitlock, C., 1998. Paleoclimate simulations for North America over the past 21,000 years: features of the simulated climate and comparisons with paleoenvironmental data. Quaternary Science Reviews 17, 549–585.

Benito, G., O'Connor, J.E., 2003. Number and size of last-glacial Missoula floods in the Columbia river valley between the Pasco basin, Washington, and Portland, Oregon. Geological Society of America Bulletin 115, 624–638.

Berger, G.W., Busacca, A.J., 1995. Thermoluminescence dating of late Pleistocene loess and tephra from eastern Washington and southern Oregon and implications for the eruptive history of Mount St. Helens. Journal of Geophysical Research 100, 22,361–22,374.

Berger, G.W., Easterbrook, D.J., 1993. Thermoluminescence dating tests of lacustrine, glaciomarine, and floodplain sediments from western Washington and British Columbia. Canadian Journal of Earth Science 30, 1815–1828.

Bjornstad, B.N., Fecht, K.R., Pluhar, C.J., 2001. Long history of pre-Wisconsin, Ice Age cataclysmic floods: evidence from southeastern Washington State. Journal of Geology 109, 695–713.

Blinnikov, M., Busacca, A., Whitlock, C., 2002. Reconstruction of the late Pleistocene grassland of the Columbia basin, Washington, USA, based on phytolith records in loess. Palaeogeography Palaeoclimatololgy Palaeoecology 177, 77–101.

Blunt, D.J., Easterbrook, D.J., Rutter, N.W., 1987. Chronology of Pleistocene sediments in the Puget lowland, Washington. In: Schuster, J.E. (Ed.), Selected Papers on the Geology of Washington. Washington Division of Geology and Earth Resources Bulletin, vol. 77, pp. 321–353.

Booth, D.B., Troost, K.G., Clague, J.J., Waitt, R.B., 2004. The Cordilleran ice sheet. In: Gillespie, A.R., Porter, S.C., Atwater, B.F. (Eds.), The Quaternary Period in the United States. Elsevier, Amsterdam, pp. 17–43.

Bretz, J.H., 1923. The channeled scablands of the Columbia plateau. Journal of Geology 31, 617–649.

Bretz, J.H., 1932. The Grand Coulee. In: American Geographical Society Special Publication, vol. 15.

Bretz, J.H., 1969. The Lake Missoula floods and the channeled scabland. Journal of Geology 77, 505–543.

Briner, J.P., Kaufman, D.S., Manley, W.F., Finkel, R.C., Caffee, M.W., 2005. Cosmogenic exposure dating of late Pleistocene moraine stabilization in Alaska. Geological Society of America Bulletin 117, 1108–1120.

Bryan, K., 1927. The Palouse soil problem. United States Geological Survey Bulletin 790, 21–46.

Busacca, A.J., 1989. Long Quaternary record in eastern Washington, U.S.A., interpreted from multiple buried paleosols in loess. Geoderma 45, 105–122.

Busacca, A.J., McDonald, E.V., 1994. Regional sedimentation of late Quaternary loess on the Columbia plateau: sediment source areas and loess distribution patterns. Washington Division of Geology and Earth Resources Bulletin vol. 80, 181–190.

Busacca, A.J., Nelstead, K., McDonald, E.V., Purser, M., 1992. Correlation of distal tephra layers in loess in the channeled scabland and Palouse of Washington State. Quaternary Research 37, 281–303.

Clague, J.J., 1989. Quaternary geology of the Canadian cordillera. In: Fulton, R.J. (Ed.), Quaternary Geology of Canada and Greenland. Geological Survey of Canada, Geology of Canada, vol. 1, pp. 17–96.

Clague, J.J., Easterbrook, D.J., Hughes, O.L., Matthews Jr., J.V., 1992. The Sangamonian and early Wisconsin stages in western Canada and northwestern United States. In: Clark, P.U., Lea, P.D. (Eds.), The Last Interglacial-Glacial Transition in North America. Geological Society of America Special Paper, vol. 270, pp. 253–268.

Clague, J.J., Barendregt, R., Enkin, R.J., Foit, F.F., 2003. Paleomagnetic and tephra evidence for tens of Missoula floods in southern Washington. Geology 31, 247–250.

Clynne, M.A., Calvert, A.T., Wolfe, E.W., Evarts, R.C., Fleck, R.J., Lanphere, M.A., 2008. The Pleistocene Eruptive History of Mount St. Helens, Washington, from 300,000 to 12,800 Years Before Present. U.S. Geological Survey Professional Paper 1750, 593–627 pp.

COHMAP Members, 1988. Climatic changes of the last 18,000 years: observations and model simulations. Science 241, 1043–1052.

Colman, S.M., Pierce, K.L., 1992. Varied records of early Wisconsinan alpine glaciation in the Western United States derived from weathering-rind thickness. In: Clark, P.U., Lea, P.D. (Eds.), The Last Interglacial-Glacial Transition in North America. Geological Society of America Special Paper, vol. 270, pp. 269–278.

Cosma, T., Hendy, I., Chang, A., 2008. Chronological constraints on Cordilleran ice sheet glaciomarine sedimentation from core MD02-2496 off Vancouver Island (western Canada). Quaternary Science Reviews 27, 941–955.

Easterbrook, D.J., 1994. Chronology of pre-late Wisconsin Pleistocene sediments in the Puget lowland, Washington. In: Lasmanis, R., Cheney, E.S. (Eds.), Regional Geology of Washington State. Washington Division of Geology and Earth Resources Bulletin, vol. 80, pp. 191–206.

Flemal, R.C., Odom, I.E., Vail, R.G., 1972. Stratigraphy and origin of the paha topography of northwestern Illinois. Quaternary Research 2, 232–243.

Franke, R., 1982. Smooth interpolation of scattered data by local thin plate splines. Computer and Mathematics with Applications 8, 273–281.

Frazee, C.J., Fehrenbacher, J.B., Krumbein, W.C., 1970. Loess distribution from a source. Proceedings – Soil Science Society of America 34, 296–301.

Fulton, R.J., Smith, G.W., 1978. Late Pleistocene stratigraphy of south-central British Columbia. Canadian Journal of Earth Science 15, 971–980.

Gaylord, D.R., Stetler, L.D., 1994. Eolian-climatic thresholds and sand dunes at the Hanford site, south-central Washington, U.S.A. Journal of Arid Environments 28, 95–116.

Gaylord, D.R., Foit Jr., F.F., Schatz, J.K., Coleman, A.J., 2001. Smith canyon dune field, Washington, U.S.A.: relation to glacial outburst floods, the Mazama eruption, and Holocene paleoclimate. Journal of Arid Environments 47, 403–424.

Gaylord, D.R., Busacca, A.J., Sweeney, M.R., 2003. The Palouse loess and the channeled scabland: a paired Ice-Age geologic system. In: Easterbrook, D.J. (Ed.), Quaternary Geology of the United States. INQUA 2003 Field Guide Volume, pp. 123–134.

Gaylord, D.R., Foit Jr., F.F., Anfinson, O., 2011. Tephrochronology of late Pleistocene and Holocene sand dune deposits, Hanford reach national monument, WA. Geological Society of America Abstracts with Programs 43, 272.

Gile, L.H., Peterson, F.F., Grossman, R.B., 1966. Morphological and genetic sequences of carbonate accumulation in desert soils. Soil Science 101, 347–360.

Hanson, M.A., Lian, O.B., Clague, J.J., 2012. The sequence and timing of large late Pleistocene floods from glacial Lake Missoula. Quaternary Science Reviews 31, 67–81.

Hooper, P.R., 2000. Chemical discrimination of Columbia river basalt flows. Geochemistry Geophysics Geosystems 1. no. 2000GC000040.

Hostetler, S.W., Bartlein, P.J., 1999. Simulation of the potential responses of regional climate and surface processes in western North America to a canonical Heinrich event. In: Clark, P.U., Webb, R.S., Keigwin, L.D. (Eds.), Mechanisms of Global Climate Change at Millennial Time Scales. American Geophysical Union Geophysical Monograph, vol. 112, pp. 313–327.

Johnson, D.M., Hooper, P.R., Conrey, R.M., 1999. XRF analysis of rocks and minerals for major and trace elements on a single low dilution Li-tetraborate fused bead. Advances in X-ray Analysis 41, 843–867.

Leget, M., 1990. Loess landforms. Quaternary International 7-8, 53–61.

Lesemann, J.-E., Brennand, T.A., 2009. Regional reconstruction of subglacial hydrology and glaciodynamic behavior along the southern margin of the Cordilleran ice sheet in British Columbia, Canada and northern Washington State, USA. Quaternary Science Reviews 28, 2420–2444.

Lewis, P., 1960. Linear topography in the southwestern Palouse, Washington-Oregon. Annals of the Association of American Geographers 50, 98–111.

Lindsey, K.A., Gaylord, D.R., 1990. Lithofacies and sedimentology of the Miocene-Pliocene ringold formation, Hanford site, south-central Washington. Northwest Science 64, 165–180.

Loeppert, R.H., Inskeep, W.P., 1996. Iron. In: Methods of Soil Analysis, Part 3. Soil Science Society of America Book Series, vol. 5, Madison, WI, 639–664 pp.

Lopes, C., Mix, A.C., 2009. Pleistocene megafloods in the northeast Pacific. Geology 37, 79–82.

Machette, M., 1985. Calcic soils of the southwestern United States. In: Weide, D.L. (Ed.), Soils and Quaternary Geology of the Southwestern United States. Geological Society of America Special Paper, vol. 203, pp. 1–21.

Marshall, S.J., Tarasov, L., Clarke, G.K.C., Peletier, W.R., 2000. Glaciological reconstruction of the Laurentide ice sheet: physical processes and modeling challenges. Canadian Journal of Earth Science 37, 769–793.

Martinson, D.G., Pisias, N.G., Hays, J.D., Imbire, J., Moore, T.C., Shackleton, N.J., 1987. Age and the orbital theory of the ice ages: development of a high-resolution 0 to 300,000-year chronostratigraphy. Quaternary Research 27, 1–30.

Marx, S.K., Kamber, B.S., McGowan, H.A., 2005. Provenance of long-traveled dust determined with ultra-trace-element composition: a pilot study with samples from New Zealand glaciers. Earth Surface Processes and Landforms 30, 699–716.

Mason, J.A., 2001. Transport direction of Peoria loess in Nebraska and implications for loess sources on the central Great Plains. Quaternary Research 56, 79–86.

Mason, J.A., Nater, E.A., Hobbs, H.C., 1994. Transport direction of Wisconsinan loess in southeastern Minnesota. Quaternary Research 41, 44–51.

Mason, J.A., Sweeney, M.R., Hanson, P.R., 2011. Evidence for eolian remobilization of loess in the central Great Plains, USA, and implications for paleoclimatic interpretation of the loess record. Geophysical Research Abstracts 13. EGU2011–3951.

McDaniel, P.A., Hipple, K.W., 2010. Mineralogy of loess and volcanic ash eolian mantles in Pacific Northwest (USA) landscapes. Geoderma 154, 438–446.

McDonald, E.V., 1987. Correlation and interpretation of the stratigraphy of the Palouse loess of eastern Washington. M.S. Thesis, Washington State University, Pullman, 218 pp..

McDonald, E.V., Busacca, A.J., 1988. Record of pre-late Wisconsin giant floods in the channeled scabland interpreted from loess deposits. Geology 16, 728–731.

McDonald, E.V., Busacca, A.J., 1989. Record of pre-late Wisconsin floods and late Wisconsin flood features in the Cheney-Palouse scabland: trip C. In: Joseph, N.L. (Ed.), Geologic Guidebook for Washington and Adjacent Areas. Washington Division of Geology and Earth Resources Information Circular, vol. 86, pp. 337–346.

McDonald, E.V., Busacca, A.J., 1990. Interaction between aggrading geomorphic surfaces and the formation of a late Pleistocene paleosol in the Palouse loess of eastern Washington State. Geomorphology 3, 449–470.

McDonald, E.V., Busacca, A.J., 1992. Late Quaternary stratigraphy of loess in the channeled scabland and Palouse of Washington State. Quaternary Research 38, 141–156.

McDonald, E.V., Busacca, A.J., 1998. Unusual timing of regional loess sedimentation triggered by glacial outburst flooding in the Pacific Northwest US. In: Busacca, A.J. (Ed.), Dust Aerosols, Loess Soils and Global Change. Washington State University College of Agriculture and Home Economics MISC0190, pp. 163–166.

McFadden, L.D., Hendricks, D.M., 1985. Changes in the content and composition of pedogenic iron oxyhydroxides in a chronosequence of soils in southern California. Quaternary Research 23, 189–204.

Mitas, L., Mitasova, H., 1988. General variational approach to the interpolation problem. Computer and Mathematics with Applications 16, 983–992.

Mix, A.C., 1992. The marine oxygen isotope record: constraints on timing and extent of ice growth events (120–65 ka). In: Clark, P.U., Lea, P.D. (Eds.), The Last Interglacial–Glacial Transition in North America. Geological Society of America Special Paper, vol. 270, pp. 19–30.

Muhs, D.R., 1992. The last interglacial-glacial transition in North America: evidence from uranium dating of coastal deposits. In: Clark, P.U., Lea, P.D. (Eds.), The Last Interglacial–Glacial Transition in North America. Geological Society of America Special Paper, vol. 270, pp. 31–51.

Muhs, D.R., Benedict, J.B., 2006. Eolian additions to late Quaternary alpine soils, Indian Peaks Widerness area, Colorado Front range. Arctic, Antarctic, and Alpine Research 38, 120–130.

Muhs, D.R., Bettis III, E.A., 2003. Quaternary loess-paleosol sequences as examples of climate-driven sedimentary extremes. In: Chan, M.A., Archer, A.W. (Eds.), Extreme Depositional Environments: Mega End Members in Geologic Time. Geological Society of America Special Paper, vol. 370, pp. 53–74.

Muhs, D.R., Budahn, J.R., Johnson, D.L., Reheis, M., Beann, J., Skipp, G., Fisher, E., Jones, J.A., 2007. Geochemical evidence for airborn dust additions to soils in Channel Islands National Park, California. Geological Society of America Bulletin 120, 106–126.

Muhs, D.R., Bettis III, E.A., Aleinikoff, J.N., McGeehin, J.P., Beann, J., Skipp, G., Marshall, B.D., Roberts, H.M., Johnson, W.C., Benton, R., 2008. Origin and paleoclimatic significance of late Quaternary loess in Nebraska: evidence from stratigraphy, chronology, sedimentology, and geochemistry. Geological Society of America Bulletin 120, 1378–1407.

Mullineaux, D.R., 1986. Summary of pre-1980 tephra-fall deposits from Mount St Helens, Washington State, USA. Bulletin of Volcanology 48, 17–26.

Mullineaux, D.R., Wilcox, R.E., Ebaugh, W.F., Fryxell, R., Rubin, M., 1978. Age of the last major scabland flood of the Columbia plateau in eastern Washington. Quaternary Research 10, 171–180.

Newcomb, R.C., 1958. Ringold formation of Pleistocene age in the type locality, the White Bluffs, Washington. American Journal of Science 256, 328–340.

Normark, W.R., Reid, J.A., 2003. Extensive deposits on the Pacific plate from late Pleistocene North American lake outbursts. Journal of Geology 111, 617–637.

O'Connor, J.E., Baker, V.R., 1992. Magnitudes and implications of peak discharges from glacial Lake Missoula. Geological Society of America Bulletin 104, 267–279.

O'Geen, A.T., Busacca, A.J., 2001. Faunal burrows as indicators of paleo-vegetation in eastern Washington, USA. Palaeogeography Palaeoclimatology Palaeoecology 169, 23–37.

Patton, P.C., Baker, V.R., 1978. New evidence for pre-Wisconsin flooding in the channeled scabland of eastern Washington. Geology 6, 567–571.

Pluhar, C.J., Bjornstad, B.N., Reidel, S.P., Coe, R.S., Nelson, P.B., 2006. Magnetostratigraphic evidence from the cold creek bar for onset of ice-age cataclysmic floods in eastern Washington during the Early Pleistocene. Quaternary Research 65, 123–135.

Porter, S.C., 1981. Use of tephrochronology in the Quaternary geology of the United States. In: Self, S., Sparks, R. (Eds.), Tephra Studies. Reidel, Boston, pp. 135–160.

Porter, S.C., Swanson, T.W., Caffee, M.W., Finkel, R.C., 2005. Cl-36 dating of the Pleistocene glacial record in the icicle creek drainage, Cascade Range, Washington. Geological Society of America Abstracts with Programs 37, 41.

Prytulak, J., Vervoort, J.D., Plank, T., Yu, C., 2006. Astoria fan sediments, DSDP site 174, Cascadia Basin: Hf-Nd-Pb constraints on provenance and outburst flooding. Chemical Geology 233, 276–292.

Pye, K., 1987. Aeolian Dust and Dust Deposits. Academic Press, London.

Pye, K., 1995. The nature, origin and accumulation of loess. Quaternary Science Reviews 14, 653–667.

Richardson, C.A., McDonald, E.V., Busacca, A.J., 1997. Luminescence dating of loess from the northwest United States. Quaternary Science Reviews 16, 403–415.

Richardson, C.A., McDonald, E.V., Busacca, A.J., 1999. A luminescence chronology for loess deposition in Washington State and Oregon, USA. Zeitschrift fur Geomorphologie 116 (Suppl. Bd), 77–95.

Ruhe, R.V., 1983. Depositional environment of late Wisconsin loess in the midcontinental United States. In: Wright Jr., H.E., Porter, S.C. (Eds.), 1983. Late-Quaternary Environments of the United States, vol. 1. University of Minnesota Press, Minneapolis, pp. 130–137.

Shao, Y., Raupach, M.R., Findlater, P.A., 1993. Effect of saltation bombardment on the entrainment of dust by wind. Journal of Geophysical Research 98 (D7), 12719–12726.

Shaw, J., Munro-Stasiuk, M., Sawyer, B., Beaney, C., Etienne Lesemann, J., Musacchio, A., Rains, B., Young, R., 1999. The channeled scabland: back to Bretz? Geology 27, 605–608.

Spencer, P.K., Knapp, A.N., 2010. New stratigraphic markers in the late Pleistocene Palouse loess: novel fossil gastropods, absolute age constraints and non-aeolian facies. Sedimentology 57, 41–52.

Sperazza, M., Moore, J.M., Hendrix, M.S., 2004. High-resolution particle size analysis of naturally occurring very fine-grained sediment through laser diffractometry. Journal of Sedimentary Research 74, 736–743.

Sun, J., 2002. Provenance of loess material and formation of loess deposits on the Chinese Loess Plateau. Earth and Planetary Science Letters 203, 845–859.

Sweeney, M.R., Busacca, A.J., Richardson, C.A., Blinnikov, M.S., McDonald, E.V., 2004. Glacial anticyclone recorded in Palouse loess of northwestern USA. Geology 32, 705–708.

Sweeney, M.R., Busacca, A.J., Gaylord, D.R., 2005. Topographic and climatic influences on accelerated loess accumulation since the last glacial maximum in the Palouse, Pacific Northwest, USA. Quaternary Research 63, 261–273.

Sweeney, M.R., Gaylord, D.R., Busacca, A.J., 2007. The evolution of eureka flat: a dust producing engine of the Palouse loess, USA. Quaternary International 162,163, 76–96.

Taylor, S.R., McLennan, S.M., 1985. The Continental Crust: Its Composition and Evolution. Blackwell Scientific, Oxford.

Troost, K.G., Booth, D.B., Mahan, S.A., Hagestrum, J.T., 2003. Presence of mid Pleistocene deposits (MIS 4 through 8) in the Tacoma area: did the possession glacier make it to Tacoma? Geological Society of America Abstracts with Programs 35, 215.

Waitt, R.B., 1985. Case for periodic, colossal jökulhlaups from Pleistocene glacial lake Missoula. Geological Society of America Bulletin 96, 1271–1286.

Waitt, R.B., Thorson, R.M., 1983. The Cordilleran ice sheet in Washington, Idaho, and Montana. In: Wright Jr., H.E. (Ed.), 1983. Late Quaternary Environments of the United States, vol. 1. University of Minnesota Press, Minneapolis, pp. 53–70.

Ward, B.C., Bond, J.D., Gosse, J.C., 2007. Evidence for a 55–50 ka (early Wisconsin) glaciation of the Cordilleran ice sheet, Yukon Territory, Canada. Quaternary Research 68, 141–150.

Washington State Division of Geology and Natural Resources, 2010. Digital Geology of Washington State at 1:100,000 Scale, Version 3.0.

Whitlock, C., Sarna-Wojcicki, A.M., Bartlein, P.J., Nickman, R.J., 2000. Environmental history and tephrostratigraphy at Carp Lake, southwestern Columbia basin, Washington, U. S. A. Palaeogeography Palaeoclimatology Palaeoecology 155, 7–29.

Zdanowicz, C.M., Zielinski, G.A., Germani, M.S., 1999. Mount Mazama eruption: calendrical age verified and atmospheric impact assessed. Geology 27, 621–624.

Zuffa, G.G., Normark, W.R., Serra, F., Brunner, C.A., 2000. Turbidite mega-beds in an oceanic rift valley recording jokulhlaups of late Pleistocene glacial lakes of the western United States. Journal of Geology 108, 253–274.